

# **Quantifying Variation in Human Rib Volumetric Bone Mineral Density (vBMD) and its Relationship to Fracture**

Undergraduate Research Thesis

Presented in Partial Fulfillment to Graduate with *Research Distinction* from the School of Health  
and Rehabilitation Sciences of the Ohio State University

By

Zachary A. Haverfield

Radiologic Sciences and Therapy, Radiography and Vascular Interventional Radiology in the  
School of Health and Rehabilitation Sciences

The Ohio State University  
2019

Thesis Committee:

Dr. Randee L. Hunter

Dr. Amanda Agnew

©Copyright by Zachary A. Haverfield, 2019.  
All rights reserved

## ABSTRACT

The human body is full of structural variation, especially in the skeletal architecture of different bones. This variation is dependent on the mechanical environment of the bone and its physiological purpose, which impacts its material and geometric properties. The relationship between these properties has been investigated in previous studies, which were largely focused on the structural and material variation of human long bones (femur, radius, tibia, etc.). It is still unknown if the variation of certain material and geometric properties found in the long bones are the same in the axial skeleton. As rib fractures are a main cause of fatality in drivers in motor vehicle crashes, it is essential to understand the multivariate factors that relate to bone quality and rib fracture risk. The purpose of this study is to investigate variation in volumetric bone mineral density (vBMD) along the length of the rib, cortical section modulus at the site of fracture (Z), and their relationship to structural properties to better understand differential fracture risk.

In total, forty-six *ex vivo* mid-level ribs (5th-7th) were obtained from n=46 post mortem human subjects (PMHS) with ages ranging from 13-83 years. The 46 PMHS were divided into two different sub-samples, the *age-matched sample* and the *physically tested sample*, which was dependent on if the rib had been dynamically tested. Each rib was scanned using a 64 slice Philips Ingenuity Computed Tomography scanner (CT) at a consistent in-plane resolution of 0.167mm. Each rib was then dynamically tested in a 2-D bending scenario to simulate anterior-posterior thoracic impact. To investigate variation along the length of the rib, Phillips Intellispace, Dataviewer, and Skyscan CTAn software (Bruker) were used to calculate a vBMD value for volumes of interest (VOIs) located at the 30%, 50%, and 75% of total rib curve length (Cv.Le), the *age-matched sample* (n=44), as well as the location of fracture for the *physically*

*tested sample* of the ribs ( $n=30$ ). Z was collected from histological cross-sections taken from the site of fracture after dynamic testing. Finally, the sub-sample's vBMD and Z were used to determine and calculate the Stress Strain Index (SSI) of the ribs.

All data collected were normally distributed ( $p>0.15$ ). One-way ANOVA demonstrated significantly different vBMD at all of the sites, 30% and the 50% sites ( $p<0.01$ ), 50% and the 75% sites ( $p<0.01$ ), and the 30% to the 75% site ( $p<0.01$ ). The 30%, 50%, and the 75% sites were statistically tested against structural properties related to the rib, Linear Structural Stiffness (K), Total Energy ( $U_{TOT}$ ), and Peak Force ( $F_{PEAK}$ ). Using a linear regression, the 50% and 75% sites showed no significant predictability with any of these factors ( $p>0.05$ ) as well as the first fracture site vBMD. The 30% site demonstrated no significant predictability between K or  $U_{TOT}$  ( $p>0.05$ ) but did demonstrate statistical significance when compared to  $F_{PEAK}$  ( $p<0.05$ ). When combining the fracture site vBMD with the fracture site Z, we were able to produce a multivariate factor, SSI. When compared to the structural properties, SSI was able to significantly predict  $U_{TOT}$ ,  $F_{PEAK}$ , and K explaining large amounts of variation within the sample ( $p<0.001$ ). However, Z alone explained slightly more variation within the sample than SSI could, excluding  $U_{TOT}$  ( $p<0.0001$ ).

Quantifying vBMD along the length of the rib shows significant variation and is an essential part of understanding and predicting rib fracture risk. Likely, generalized scores are not enough to quantify and determine whole bone quality. Utilizing multifactor variables may prove useful in future analysis of bone quality assessment.

## ACKNOWLEDGEMENTS

This project owes a large majority of its completion to the Injury Biomechanics Research Center (IBRC), the Skeletal Biology Research Laboratory (SBRL), and their accompanying faculty and staff. Overseen by Dr. Amanda Agnew and Dr. John Bolte, the IBRC and the SBRL have welcomed undergraduate and graduate students to pursue their interest in research and science for years. The positive environment that they, and all of the members and volunteers in the laboratory, have created has been largely beneficial to not only the research I have been conducting, but to many other students as well.

One of the greatest gifts to research is through body donation. The Ohio State University's Body Donor Program and Lifeline of Ohio provide the IBRC with donors who have selflessly chosen to give their bodies to science and research. I would like to thank each donor in this project including their families and friends. Without their acts of generosity and courage, the research of this project and many others would be impossible.

I would also like to thank my advisor, Dr. Randee Hunter for her willingness to teach and encourage me throughout this process. Without her guidance and expertise, this project would not be where it currently is today. Additionally, I would like to thank Dr. Karen Briley who has helped immensely in the organization of imaging data and in imaging analysis. Finally, I would like to thank Dr. Amanda Agnew and Dr. Randee Hunter individually for their help with forming the ideas for this project and for their insight into the project's proposal and its finalization. As a graduating senior, I am grateful for the opportunity that you have given me this past year and because of your generosity and dedication to teaching, you have guided and shaped my education in ways I never thought possible.

# TABLE OF CONTENTS

<b>ABSTRACT.....</b>	<b>3</b>
<b>ACKNOWLEDGEMENTS .....</b>	<b>5</b>
<b>LIST OF TABLES.....</b>	<b>7</b>
<b>LIST OF FIGURES.....</b>	<b>8</b>
<b>INTRODUCTION .....</b>	<b>9</b>
<b>LITERATURE REVIEW .....</b>	<b>13</b>
<b>MATERIALS AND METHODOLOGY .....</b>	<b>17</b>
<i>Population and Sample.....</i>	<i>17</i>
<i>Rib Procurement and Initial Scanning .....</i>	<i>17</i>
<i>2D Dynamic Loading Test .....</i>	<i>18</i>
<i>Computed Tomography Analysis .....</i>	<i>19</i>
<b>RESULTS .....</b>	<b>25</b>
<b>DISCUSSION .....</b>	<b>34</b>
<i>Variation of vBMD within the Rib .....</i>	<i>34</i>
<i>Overall lack of vBMD Predictability to Structural Properties.....</i>	<i>34</i>
<i>Insignificance of Fracture Site vBMD to Structural Properties.....</i>	<i>35</i>
<i>Analysis of Fracture Site Z and Structural Properties .....</i>	<i>35</i>
<i>Differences in Fracture Site SSI and Structural Properties .....</i>	<i>36</i>
<i>Overall Conclusions.....</i>	<i>37</i>
<b>REFERENCES .....</b>	<b>39</b>
<b>APPENDIX.....</b>	<b>43</b>

## LIST OF TABLES

TABLE 1: THE DEMOGRAPHIC DATA OF THE AGE-MATCHED SAMPLE. ....	43
TABLE 2: THE DEMOGRAPHIC DATA OF THE PHYSICALLY TESTED SAMPLE. ....	44

## LIST OF FIGURES

FIGURE 1 PHILLIPS INTELLISPACE .....	20
FIGURE 2 DATAVIEWER ROTATION .....	21
FIGURE 3 SKYSCAN CTAN VOI SELECTION.....	23
FIGURE 4 30% CV.LE CORTEX DEFINING .....	23
FIGURE 5 50% CV.LE CORTEX DEFINING .....	23
FIGURE 6 75% CV.LE CORTEX DEFINING .....	24
FIGURE 7 HOUNSFIELD UNIT CALIBRATION CURVE.....	24
FIGURE 8 VBMD VARIATION BOXPLOT .....	25
FIGURE 9 VBMD VS. K SCATTERPLOT .....	26
FIGURE 10 VBMD VS UTOT SCATTERPLOT.....	27
FIGURE 11 VBMD VS. FPEAK SCATTERPLOT.....	27
FIGURE 12 FRACTURE VBMD VS. K SCATTERPLOT .....	28
FIGURE 13 FRACTURE VBMD VS $U_{TOT}$ SCATTERPLOT .....	28
FIGURE 14 FRACTURE VBMD VS. $F_{PEAK}$ SCATTERPLOT .....	29
FIGURE 15 Z VS. K SCATTERPLOT .....	30
FIGURE 16 Z VS. $U_{TOT}$ SCATTERPLOT.....	30
FIGURE 17 Z VS. $F_{PEAK}$ SCATTER PLOT.....	31
FIGURE 18 SSI VS. K SCATTERPLOT.....	32
FIGURE 19 SSI VS. $U_{TOT}$ SCATTERPLOT .....	32
FIGURE 20 SSI VS. $F_{PEAK}$ SCATTERPLOT .....	33
FIGURE 21 SSI CALCULATION EQUATION .....	44



## INTRODUCTION

The structural architecture of bone in the human body consists of vast amounts of variability in the axial and appendicular skeleton. These bones provide the body with muscle and ligament attachments, the creation of the cellular and molecular components of blood, storage sites for the majority of the body's calcium and other minerals, and allow for the protection of vital organ structures.<sup>5</sup> While there are certain consistencies throughout the structure and composition of bones in the skeletal system, each bone can differ in its makeup based upon the mechanical environment in which it resides and its physiologic purpose to the body.<sup>13</sup> Repetitive forces incurred by a bone can drastically influence its structural characteristics, including volumetric bone mineral density (vBMD) and section modulus (Z).

When considering the process of bone remodeling, we can begin to understand how prevalent this is in a bone's development, based on the bone's function in the human body. The phrase "structure determines function" is commonly used in the medical field to describe how and why the body works in certain ways and especially with consideration to the skeletal system.<sup>5,21</sup> In numerous places in the skeletal system, we can observe the results of how the structure of one bone determines the function of itself. Between the axial and appendicular skeleton, there are fundamental differences in function of the bones in each category. The appendicular skeleton consists of highly moveable and longer bones, with few exceptions such as the clavicles, scapulae, and pelvis though each provides vital structural support for limb movement. The bones in this part of the skeletal system endure large amounts of pressure and force at irregular intervals, which is why their structure must be able to support such a loading environment. The axial skeleton, however, is comprised of many bones that are primarily utilized for protection and structural integrity. For instance, spinal vertebral bodies are used for both

constant structural support and the protection of the spinal cord and other sensitive anatomy. Rib bones provide protection of the thoracic and part of the abdominal cavities. However, they too undergo a cyclic force that expands and contracts the thoracic cavity, ventilation. Although all bone in the human body is comprised of similar materials, a bone's ability to adapt and change, based upon the regular or irregular forces that it is impacted by, allows for specialization and creates variation throughout the body.<sup>5,21</sup>

Variation within a bone is essential in determining its strength and resistance to fracture, as some bones are made for different physiological reasons. One of the ways that bone can vary is through its classification of being brittle or ductile. The precise amount of materials in bone determine the bone's ability to resist and transfer forces that it undergoes. Mineralization in bone is one way that bone strength and resistance to fracture is currently defined and occurs when type 1 collagen is secured by a calcium hydroxyapatite crystalline structure made up of phosphorus and calcium.<sup>24</sup> This concentration of collagen and its crystalline support must be precisely distributed depending on the bone. If mineralization in the bone is too little, then the result would be a bone that would not be as stiff but has increased flexibility.<sup>20,21</sup> However, this could lead to bone structural failure easier than it would if the correct amount of mineralization was used. Conversely, if the mineralization of the bone is too great, then the bone would have diminished flexibility and be extremely brittle, which could also result in fracture. The correct balance of these factors results in a bone that is not only stiff and sturdy, but also able to distribute pressure, weight, and other forces with its inclined flexibility. Depending on the bone, this ratio of mineralization could vary to suit its purpose.<sup>2,10,21</sup> For instance, the ribs, being under constant cyclic expansion and contraction, may have a lower ratio of mineralization than the femur, as ribs need more flexibility due to movement involved in ventilation. This distribution of bone

mineralization, composed of calcium hydroxyapatite, is clinically measured as the bone mineral density (BMD) and is used in calculating the strength and fracture resistance of a given bone.<sup>2,10,21</sup>

Currently, assessing bone quality, strength, and diseases that impact these factors like osteoporosis is commonly done through dual-energy X-ray absorptiometry (DXA). This method utilizes x-radiation and an image receptor plate to determine how much radiation is able to penetrate the bone and reach the receptor. Depending on the tissue thickness, and density of the material, x-rays are absorbed differently throughout the body. The amount of radiation that is absorbed by certain densities of calcium hydroxyapatite results in areal bone mineral density (aBMD) value used in comparison to a reference population to create a T-score that represents the individual's risk of fracture.<sup>4,7,25</sup> aBMD is thought to represent the amount of mineralization within the bone as a proxy measurement. However, some of the issues this method are that patients are placed into simplified T-score categories where little to no variation within the skeleton or bone itself is taken into account. The categorical determination of the patient's score is broad, and it is unable to account for the bone as a three-dimensional object as it is compressed into a two-dimensional set of data.<sup>4,7</sup> The data that are produced are not entirely accurate when the bone is not separated out from the rest of the anatomy. Anatomical variation such as vessel calcification, hyperdense epithelial tissue, and mineral deposits outside of the bone can all skew the results of the DXA scan.<sup>4,7</sup> These scans also do not demonstrate how the mineralization is distributed throughout the bone, which is an essential factor for the bone to have a correct ratio of stiffness and flexibility.

Quantitative Computed Tomography (QCT) allows for the three-dimensional reconstruction of bone, unlike DXA scanning. Measuring volumetric BMD (vBMD) using QCT

allows for individual segmentation and analysis of bone without the negative implications that are inherent in DXA. Utilizing QCT, a single cross-section or a specific volume of interest (VOI) is captured and analyzed for three-dimensional data collection.<sup>8,9</sup> This method especially helps with the analysis of the bone's cortex and is able to obtain data on the vBMD of the desired location, allowing for the analysis along different points in a bone's length.<sup>18</sup> When vBMD at certain locations is calculated, variations in BMD along the length of the bone can be detected for a more rounded and comprehensive understanding of the bone's make-up and of its internal structure.

The geometric construction of bone is also dependent on the bone's loading environment and the associated forces that it undergoes. Section modulus ( $Z$ ) is defined as the geometric property of bone and other beam-like structures.<sup>19</sup> It is a mathematical calculation that takes the moment of inertia ( $I_z$ ) around a given axis of the beam and is divided by the distance from the axis to the furthest point on the bone.<sup>19</sup> Regarding the rib, the furthest distance from the neutral axis, or centroid, can either be on the pleural side or cutaneous side of the rib's cross-section.<sup>2,19,24</sup> In combination with vBMD,  $Z$  can be used to create a multivariate factor called Stress Strain Index (SSI) which may allow for more human variation to be accounted for regarding bone strength and the assessment of bone quality.

Ribs protect many vital organ structures that are housed within the human thorax. When fractured, there is potential for the rib displacement to lacerate and inflict injury on the very structures which it serves to protect. Quantification and analysis of rib bone strength and the quality of the bone itself through vBMD,  $Z$ , and SSI can allow for a more comprehensive understanding of the differential fracture risk of ribs and can lead to factors that have the ability to predict where a fracture may occur along the rib's length.

## LITERATURE REVIEW

The ability for bone to protect and support the human body is dependent on its biological structure and its composition. Quantifying these variations to predict and further understand rib structural properties has proven to be a challenging task. **Due to minimal research and studies conducted with ribs, there are still gaps in our understanding of the factors that determine bone quality and risk of fracture, as only specific sites and variables have been studied independently.<sup>11,12</sup> By analyzing parameters along the entire length of the rib and studying how these factors relate to its structural properties, we can develop a more comprehensive understanding of bone quality and differential fracture risk in the rib than current methods.**

Ribs provide vital protection to essential organs of the thorax that are highly vascular in nature. When trauma to the rib has occurred, there is a potential for the rib to fracture and possibly lacerate or impale the organ structures that it is supposed to protect. Lien et al. (2009) conducted a study consisting of 18,856 patients that were observed during their hospital stay after being admitted for rib fractures. Of the patients that were admitted, 459 of the subjects died within twenty-four hours of admission, and it was shown that patients were at a greater risk of twenty-four-hour morbidity as the number of rib fractures increased.<sup>16,18</sup> Additionally, thoracic injuries such as rib fractures in traumatic loading scenarios have shown to increase the mortality and morbidity rate in motor vehicle crash (MVC) victims. Chest injuries have demonstrated a fatal effect in nearly 47% of drivers 65 and older and nearly double that amount for drivers 16-33 years old.<sup>2</sup> As rib fractures are a main cause of fatality in drivers in MVCs, it is essential to understand the multivariate factors that determine fracture resistance.

Currently, DXA is considered the clinical standard for assessing and quantifying BMD within a given bone. However, it has proven to be an inaccurate and flawed method of assessing the true BMD of a bone as many other factors contribute to x-ray absorption in an *in vivo* bone.

DXA relates the inaccurate BMD values it obtains to generalized and broadly categorized T-scores.<sup>4</sup> These T-Scores depict the patient's propensity to fracture by comparing the BMD of the patient to a BMD of an average young adult male or female and is then placed into three broad categories. A T-score greater than or equal to -1.0 would classify a normal individual BMD, a T-score between -1.0 and -2.5 would be classified as osteopenic, and a T-score less than or equal to -2.5 would be a bone that is thought to be osteoporotic.<sup>3,4</sup> Even with this seemingly established method of assessing bone quality, fracture risk has shown to increase independently of the determined T-score.<sup>4,7,25,26</sup>

Bone quality in ribs is comprised of a multitude of factors. Agnew et al. (2015) conducted an investigation on the effects of age and sex and their relationship to structural properties of the rib.<sup>1</sup> With 140 ribs from 70 different subjects tested, there was significant evidence supporting that age and sex are not good predictors of the structural properties of ribs.<sup>2</sup> Since these variables do not demonstrate any significant relationship to structural properties in the rib, more investigation is needed to study the factors that demonstrate an effect of the structural properties of ribs and how their variation can also have a relationship to the assessment bone quality.<sup>20,22,23</sup>

In a preliminary investigation conducted by the Injury Biomechanics Research Center, 71 subjects were examined to measure vBMD variation in mid-level ribs (5-7) on both sides of the thorax. The analysis demonstrated that there was no significant difference in cortical vBMD depending on rib level or side of the rib within subjects ( $p=0.20$  and  $p=0.93$ ).<sup>12</sup> This indication that there is no variation in cortical vBMD between rib level and different sides of an individual subject allows for ribs to be used from either side and multiple mid-rib levels.<sup>12</sup> Stress strain index (SSI) was also analyzed in this study. This index number constructed from vBMD and Z

makes it a combination variable. This preliminary investigation demonstrated that a strong relationship between SSI and total force, peak force ( $F_{PEAK}$ ), and stiffness ( $K$ ) at 50% of the rib's Cv.Le. for each structural property ( $p < 0.001$ ).<sup>12</sup> While these factors were determined to have significant relationships, additional information is required to understand the variation in these properties along the length of the rib and at fracture locations resulting from a loading environment.<sup>12</sup>

A previous study that has been conducted to analyze the co-variations of vBMD and Z, has been done in the tibiae at the Injury Biomechanics Research Center. This study consisted of 39 subjects with ages ranging from 25 to 87 years old. vBMD demonstrated inverse relationships were found between vBMD and Z along the length of the tibia.<sup>11</sup> More importantly, this illuminated the significant variation in vBMD along the length of the tibiae, at the 38%, 50%, and 66% of the bone's length.<sup>11</sup> Determining variation within a bone of the appendicular skeleton, regarding it irregular forces, brings into question whether or not such variation will be present within the rib bone of the axial skeleton.

Rib fractures pose serious threats and increased mortality rates of patients. Understanding and correctly assessing fracture risk of the ribs is essential to developing a methodology to predict and assess rib bone quality and fragility. In our current assessment of bone quality, performed through DXA scanning, there is little information about the variations in BMD related to bone strength. The data it can provide has demonstrated DXA is inherently limited and, in some respects, fundamentally flawed. Reassessing bone quality through QCT and its variations can provide key insight into rib bone quality and fracture resistance.

The objectives of this study are:

1. Determine the variation in vBMD along the length of the rib from cross-sectional CT scans.

H<sub>0</sub>: There will not be significant differences in vBMD between the 30%, 50%, and 75% sites.

H<sub>A</sub>: There will be significant differences in vBMD between the 30%, 50%, and 75% sites.

2. Analyze the ability for vBMD along the length of the rib to predict structural properties.

H<sub>0</sub>: There will not be significant relationships between vBMD along the length of the rib and structural properties.

H<sub>A</sub>: There will be significant relationships between vBMD along the length of the rib and structural properties.

3. Analyze the ability of Z to predict rib bone structural properties at rib fracture location independent of SSI.

H<sub>0</sub>: Z will not have any statistically significant relationship to rib structural properties.

H<sub>A</sub>: Z will have a statistically significant relationship to rib structural properties.

4. Analyze the ability of SSI to predict rib bone structural properties at rib fracture location.

H<sub>0</sub>: SSI will not have any statistically significant relationship to rib structural properties.

H<sub>A</sub>: SSI will have a statistically significant relationship to rib structural properties.



# MATERIALS AND METHODOLOGY

## Population and Sample

This study is divided into two different sample sets, with some overlap between the samples. The first sample, referred to as the *age-matched sample*, is an age-matched sample of 44 post-mortem human subjects (PMHS), consisting of 22 males and 22 females. Males ages ranged from 18 to 83 years and an average age of 46.6 (+/- 18.4 years). Females ages ranged from 16 to 83 years and an average age of 46.1 (+/- 18.6 years). The *ex vivo* ribs in the sample set were comprised of 31 left ribs and 13 right ribs. Males and females in the *age-matched sample* were paired together with age differences no greater than 3 years to control for age. (See appendix: Table 1)

The second sample, referred to as the *physically tested sample*, consists of a smaller sub-sample. The sub-sample of 30 PMHS in this sample is comprised of 18 males and 12 females with ages ranging from 13 to 83 years and an average age of 43.5 (+/- 19.2). Males ages ranged from 13 to 73 and an average age of 39.7 (+/- 19.2). Females ages ranged from 16 to 83 and an average age of 49.5 (+/- 18.83). The *ex vivo* ribs in the sample set were comprised of 15 left ribs and 16 right ribs. This sample is not matched by age but does include some overlap with the age-matched sample (those that have been tested in a dynamic loading scenario). (See appendix: Table 2)

## Rib Procurement and Initial Scanning

In total, 46 PMHS were donated through either the Ohio State University Body Donor Program or Lifeline of Ohio. Each of the subjects in this study were screened to ensure that no significant trauma to the body occurred at the time of death, no initial autopsy or embalming of

the subject or inherent communicable diseases. Donors in this sample demonstrated a body mass index score (BMI) of 16-30 with a body weight ranging from 80lbs-215lbs.

For this study, each of the 46 PMHS had one mid-level rib, defined as the 5<sup>th</sup> through the 7<sup>th</sup> thoracic ribs, excised, measured for the rib's Cv.Le and wrapped in normal saline soaked gauze for storage at a consistent temperature of -20° Celsius. Each rib was individually scanned in a Phillips Ingenuity CT 64 slice scanner at consistent acquisition parameters including in-plane resolution of 0.167mm and a slice thickness of 0.671mm. In the CT scan itself, a 0.0-0.8g/cc cortical phantom (QRM) was used for Hounsfield Unit calibration during image analysis. The QRM phantom utilizes known densities of calcium hydroxyapatite which is used in defining a bone's mineral density. The known density of water was also used for image analysis calibration by using a water filled syringe in the scan itself.

## 2D Dynamic Loading Test

In order to measure and obtain structural properties of the bone, each rib in the *physically tested sample* was tested in a custom-made dynamic mechanical loading environment which utilized a specialized pendulum with a known mass of 54.4kg to initiate a 1-2m/s antero-posterior rib frontal impact.<sup>1</sup>

Each of the *ex vivo* rib's sternal and vertebral ends were placed and potted in Bondo® Body Filler and allowed to set, simulating the natural sternocostal and costovertebral joints. Four Vishay Micro-Measurement strain gauges were placed at 30% and 60% of the rib's Cv.Le on both the pleural and cutaneous surfaces of the bone. A linear string potentiometer was placed on the anterior portion of the rib to measure x-axis displacement. Finally, a Humanetics 6-axis load cell will be used to measure Linear Structural Stiffness (K), Peak Force (F<sub>PEAK</sub>), and Total

Energy ( $U_{TOT}$ ). Once the measurement devices were placed, the potted rib was testing in the custom-made structure and contracted until the rib reached failure. All the ribs that were tested reached failure. The data collected was used to construct Force-Displacement Curves for each rib (Figure 2). The site of the fracture was recorded in millimeters of the rib's Cv.Le as well as a percentage of the rib's Cv.Le. Histological cross-sections were taken adjacent to the site of fracture for section modulus calculation.<sup>1</sup>

### Computed Tomography Analysis

Each rib's CT scan was uploaded into Phillips Intellispace software. 30%, 50%, and 75% of the rib's Cv.Le was determined, with 0% being the vertebral end and 100% being the sternal end. Utilizing a multi-point measurement tool, a line was created starting from the vertebral end and terminating at the desired percentage of the rib's Cv.Le, 30%, 50%, or 75%. The axial plane was moved to the termination point of the multi-point line to determine the cross-section of that site on the rib (Figure 1).

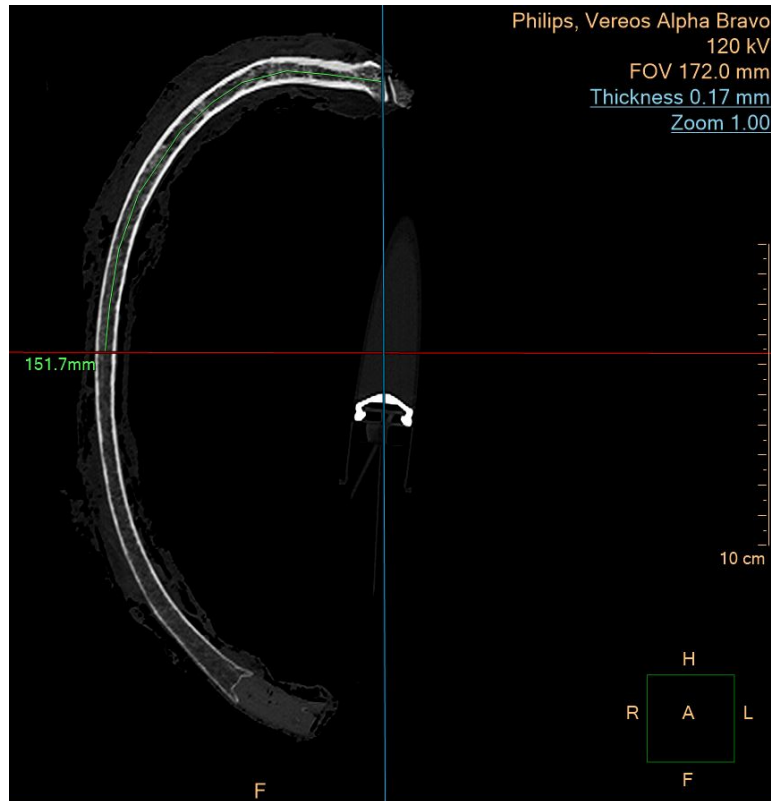
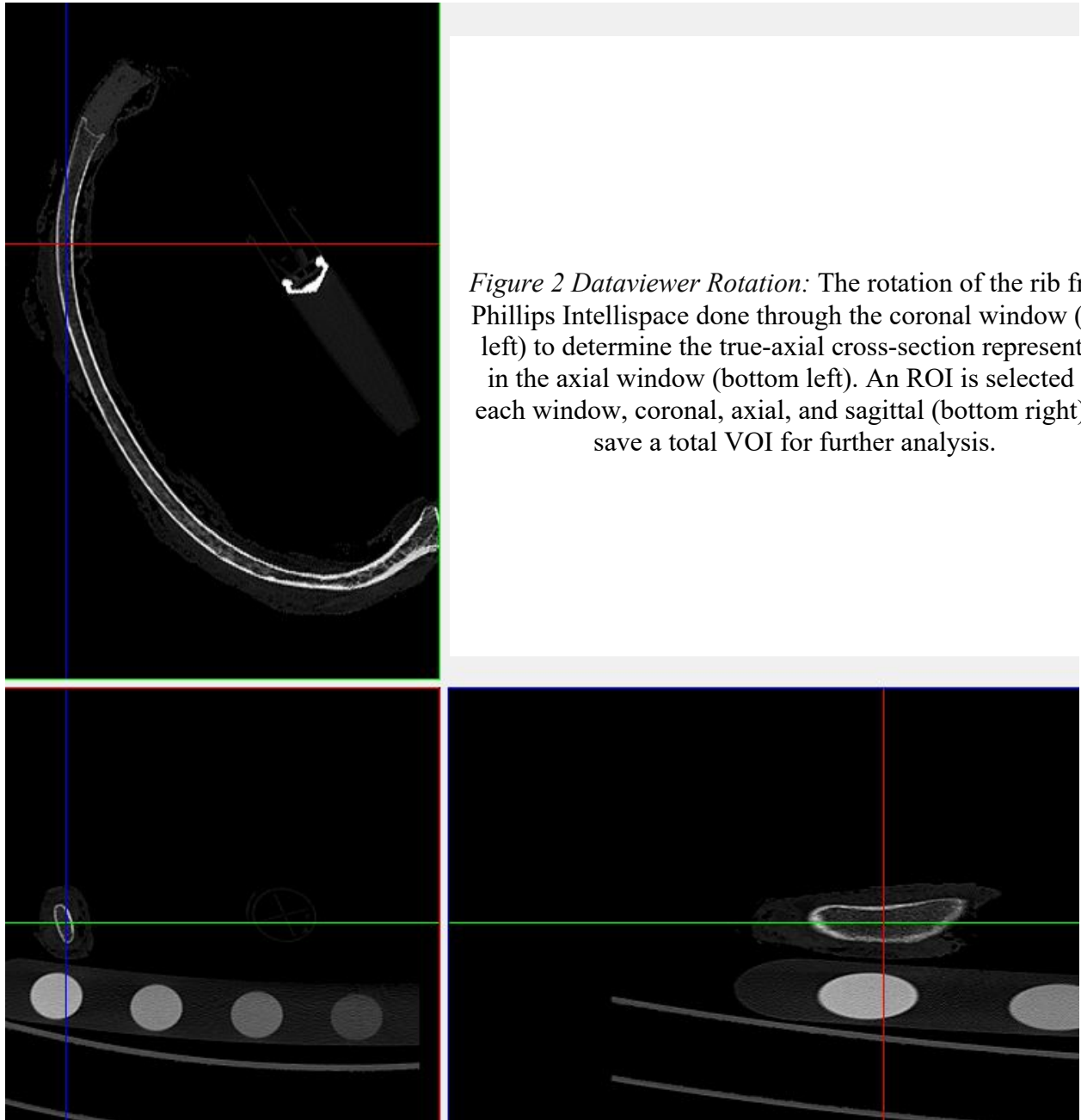


*Figure 1 Phillips Intellispace:* Measurement of the rib through the medullary cavity of the bone. The red line represents the axial plane as it crosses the bone's cortex and becomes in line with the measured multi-point line in green.

The same rib CT was then opened in Dataviewer, another program that allows for image manipulation, and the previously determined cross-section in Phillips Intellispace software was visually matched. Once the correct cross-section is matched, the image was then rotated to position the cross-section in a true axial plane, in relation to the axial window of Dataviewer. A volume of interest (VOI) outlined as much of the image as possible and it was saved for later analysis. Depending on the CT scan and the rib's curvature, the rotation of the image would occasionally result in truncation, or image cut-off, of the data. This occurs at the lower and higher percentages of the rib's Cv.Le, which is why the 30% site was used instead of the 25% site. When this did occur, the image was once again reopened, matched with Phillips Intellispace, and rotated. However, the rotation was changed to match the axial plane of the rib to the sagittal

window of Dataviewer. This allowed for the image to be rotated to a true-axial and resulted in a correction of truncated data sets and ages (Figure 2).



Once the correct, reoriented image of the CT was saved without truncated data, the dataset was opened in Skyscan CTAn software (Bruner) to analyze vBMD of the VOI at 30, 50, and 75% sites. The slice was visually matched once again, this time to the reoriented slice in Dataviewer, and a VOI was determined by taking twenty data lines above and twenty data lines below the matched slice, with the total new volume measuring 6.68mm of the rib's length. An ROI was set within the selected VOI and was used to ensure that the cross-section of the rib was isolated for analysis (Figure 3). Thresholding (148-255) was used to isolate cortical bone. A new VOI was analyzed and bounded with specific calibration ranges determined from un-thresholded water. The whole VOI was then analyzed to isolate the cortex and obtain HU values for vBMD calculation (Figures 4, 5, 6). An average HU from each slice is used to determine the average HU for the entire VOI at each site. This value that is made is then used as an input into a calibration curve (Figure 7) to produce a vBMD value. Utilizing un-thresholded water, the calibration curve scale is determined by its known density and x-ray attenuation. In order to create the calibration curve itself, which is specialized to each rib CT scan, the QRM phantom produces HU of known densities which are plotted on the curve. Once the curve has been created, the HU values of the rib VOI are then compared to this calibration curve and subsequently, the density is determined from HU. This density represents the average amount of calcium hydroxyapatite that the VOI has based upon its HU. This process was done for each of the 30%, 50%, and 75% of the rib's Cv.Le as well as location of fracture for each rib.

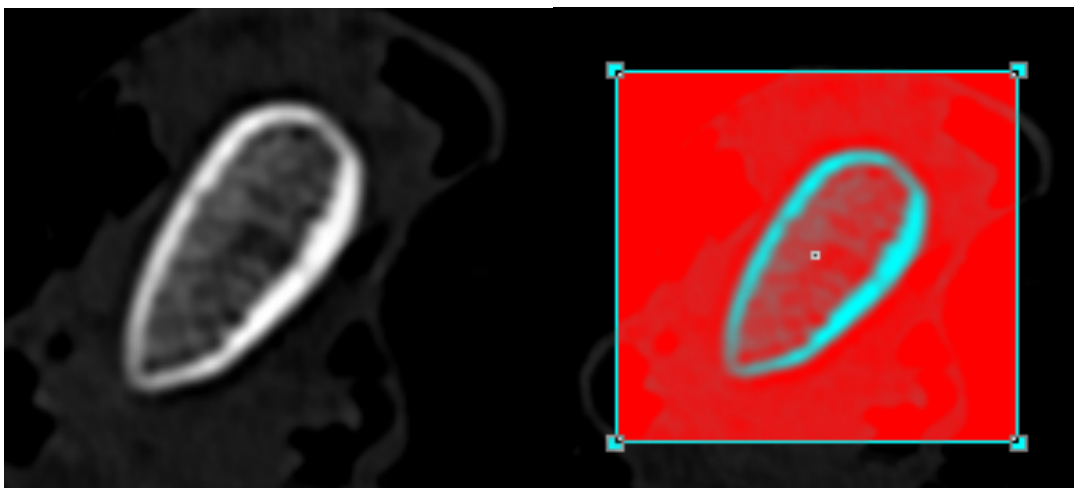


*Figure 3 Skyscan CTAn VOI Selection:* The selection of a ROI from the defined VOI around the cortex of the bone. This allows for complete isolation of the VOI without image artifact interference.

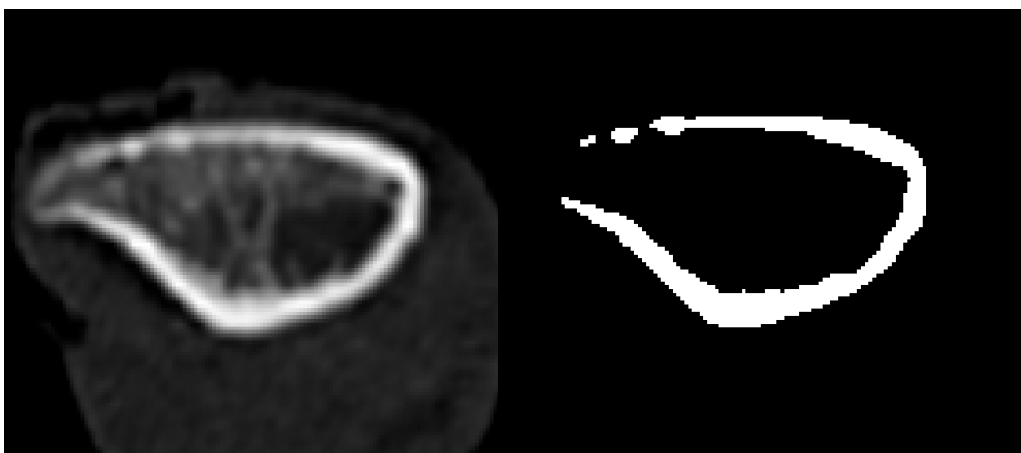


*Figure 4 30% Cv.Le Cortex Defining:* The VOI of the 30% site vBMD VOI cortex defining and analysis.

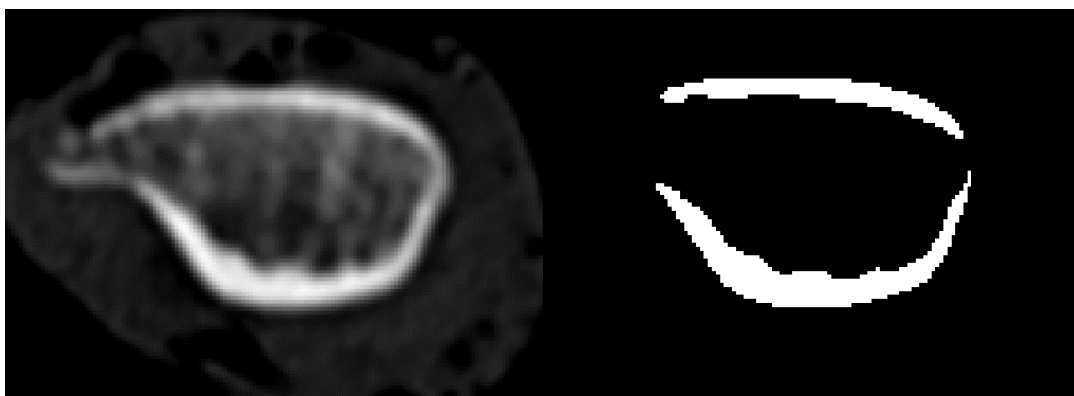


*Figure 5 50% Cv.Le Cortex Defining:* The VOI of the 50% site vBMD VOI cortex defining and analysis.

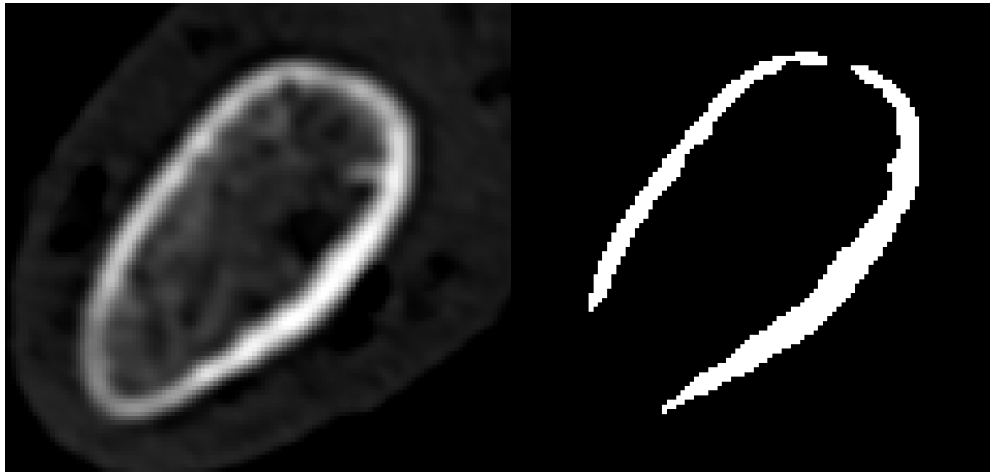


*Figure 6 75% Cv.Le Cortex Defining: The VOI of the 75% site vBMD VOI cortex defining and analysis.*

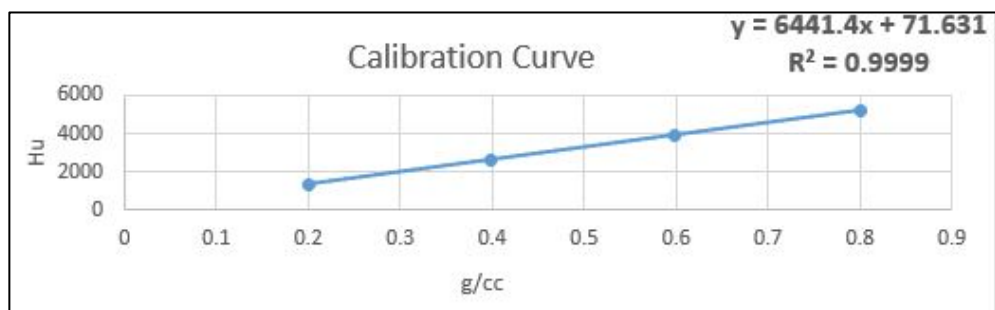


*Figure 7 Hounsfield Unit Calibration Curve: A typical calibration curve using the QRM phantom and the known density of water.*



## RESULTS

The *age-matched sample* data, which was normally distributed, was analyzed in MiniTab statistical software. For this sample, the vBMD at the 30%, 50% and 75% sites were determined and compared to each other to detect any significant differences between the varying locations along the rib's Cv.Le. Using one-way ANOVA with post hoc tests, the 30% site vBMD was compared to the 50% site vBMD and demonstrated significant differences between the two ( $p=0.002$ ). The 30% site vBMD was then compared to the 75% site vBMD and significant differences in vBMD were also detected ( $p<0.001$ ). Finally, the 50% site vBMD and the 75% site vBMD were analyzed and significant differences were also found ( $p<0.001$ ) (Figure 8).

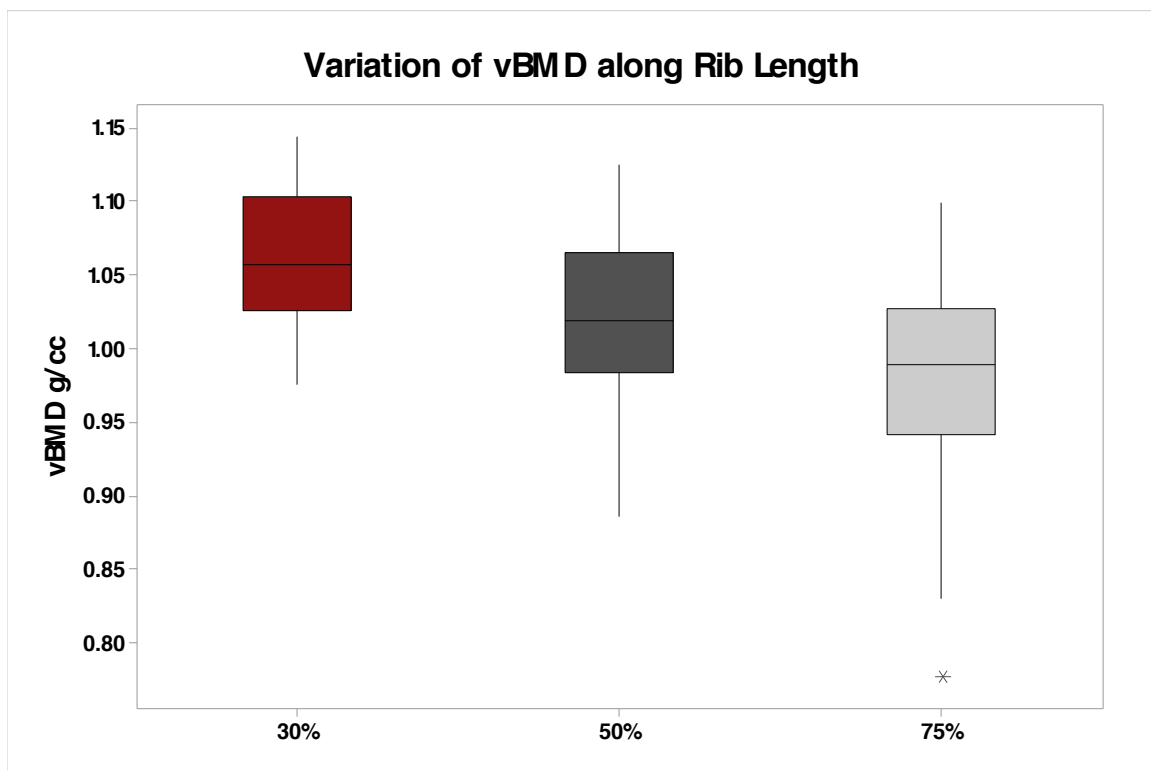


Figure 8 vBMD Variation Boxplot: Significant variation in vBMD at the 30%, 50%, and 75% Cv.Le ( $p<0.001$  for 50% and 30% compared to 75% but  $p=0.002$  for 30% to 50%).

The *physically tested sample* had the vBMD at the 30%, 50%, 75%, as well as the fracture site vBMD calculated. The fracture site's Z was also determined through histological cross-sectional analysis. To determine if the 30%, 50%, or the 75% site vBMD was able to significantly predict structural properties of the rib from the 2D Dynamic Loading Test, linear regressions were used from MiniTab statistical software as well. Comparing the 50% and the 75% site vBMD to  $U_{TOT}$ ,  $F_{PEAK}$ , and K, no significant ability to predict the structural properties was detected ( $p=0.860$ ,  $p=0.337$ , and  $p=0.481$  for 50% and  $p=0.200$ ,  $p=0.203$ , and  $p=0.451$  for 75% respectively) (Figures 9, 10). However, the 30% site vBMD was able to significantly predict  $F_{PEAK}$  ( $p=0.034$ ) but was unable to predict  $U_{TOT}$  or K ( $p=0.2$  and  $p=0.078$ ) (Figure 11). While the 30% site was able to predict  $F_{PEAK}$ , statistically speaking, it was only able to explain 14.82% of the variation within the population sample.

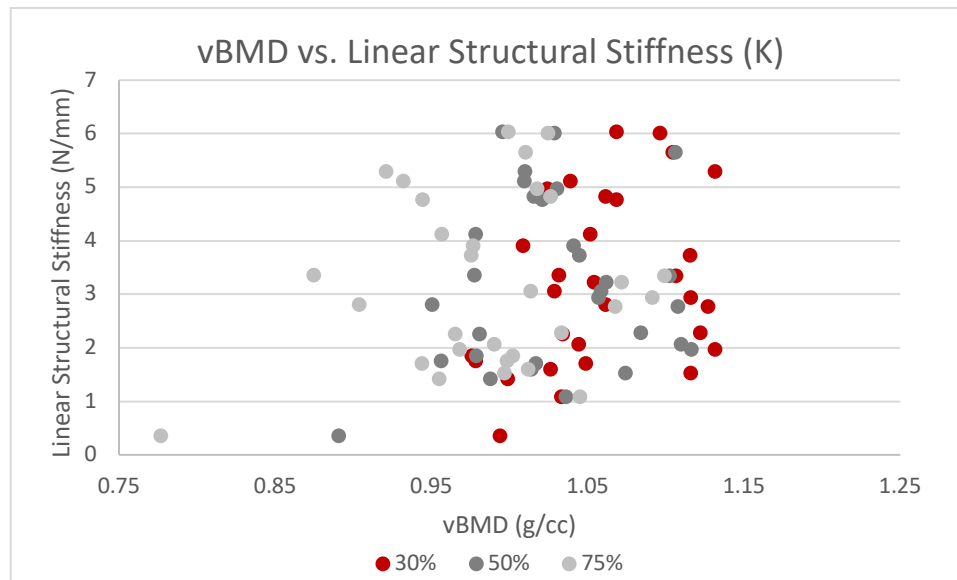


Figure 9 vBMD vs. K Scatterplot: No significant relationships between vBMD at the 30%, 50% or 75% Cv.Le when compared to K ( $p=0.078$ ,  $p=0.481$ , and  $p=0.451$ ).<sup>1</sup>

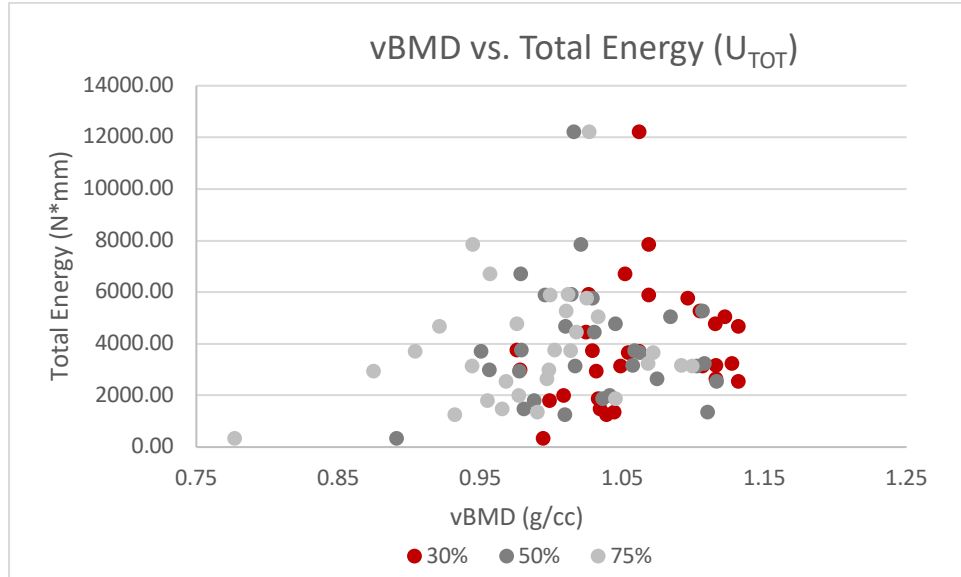


Figure 10 vBMD vs  $U_{TOT}$  Scatterplot: No significant relationships between vBMD at the 30%, 50% or 75% Cv.Le when compared to  $U_{TOT}$  ( $p=0.200$ ,  $p=0.860$ ,  $p=0.200$ ).<sup>1</sup>

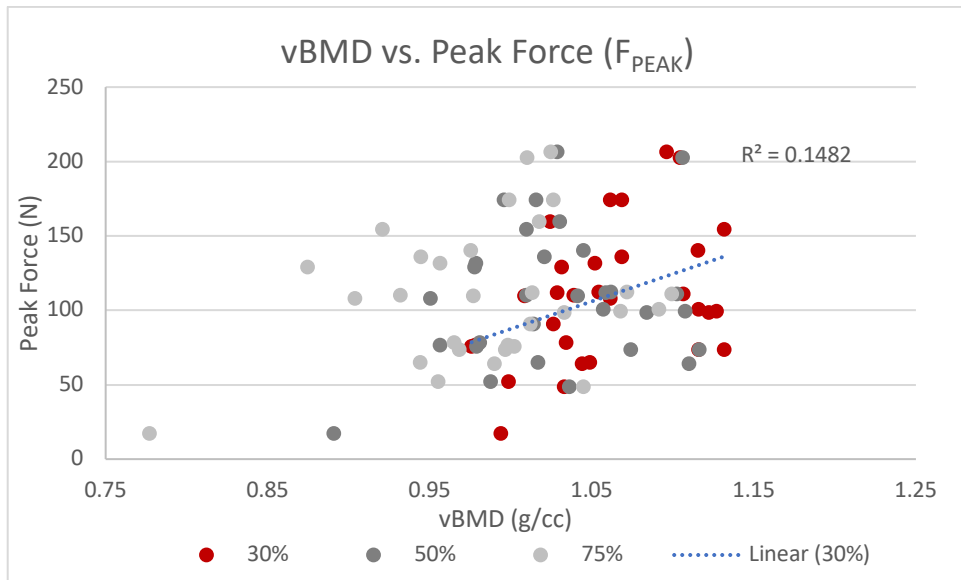


Figure 11 vBMD vs.  $F_{PEAK}$  Scatterplot: No significant relationships between vBMD at the 50% or 75% Cv.Le when compared to Peak Force ( $p=0.337$  and  $p=0.203$ ). Significant relationship between the 30% site vBMD and  $F_{PEAK}$  but only accounting for 14.82% of the population sample ( $p=0.036$ ).<sup>1</sup>

The first fracture site vBMD of the *physically tested sample* was then compared to the structural properties,  $U_{TOT}$ ,  $F_{PEAK}$ , and  $K$ . Statistical results showed that the vBMD at the fracture

site was also unable to significantly predict any of the structural properties,  $U_{TOT}$ ,  $F_{PEAK}$ , and  $K$  ( $p=0.256$ ,  $p=0.846$ , and  $p=0.392$  respectively) (Figures 12, 13, 14).

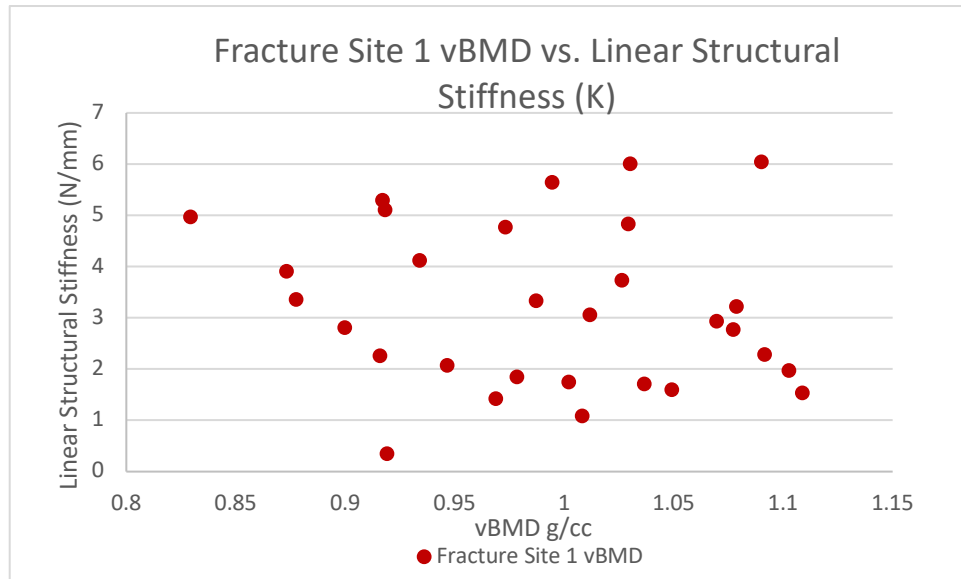


Figure 12 Fracture vBMD vs.  $K$  Scatterplot: No significant relationships between vBMD at fracture site 1 or  $K$  ( $p=0.392$ ).<sup>1</sup>

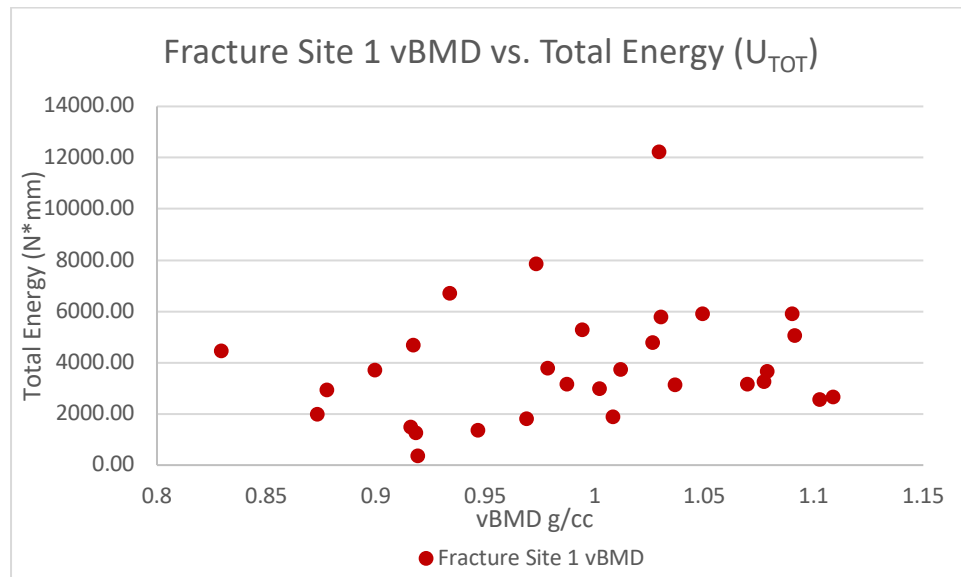
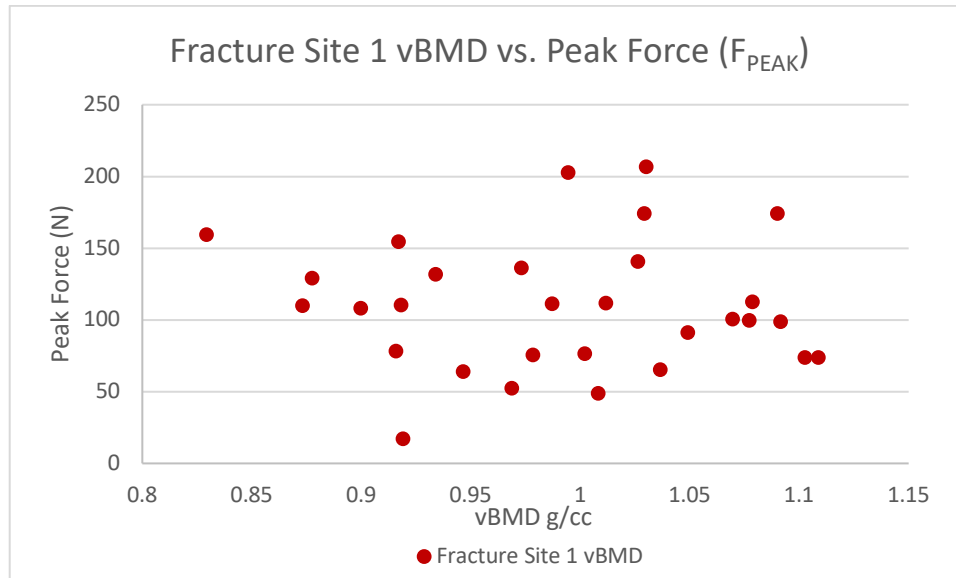


Figure 13 Fracture vBMD vs  $U_{TOT}$  Scatterplot: No significant relationships between vBMD at fracture site 1 or  $U_{TOT}$  ( $p=0.256$ ).<sup>1</sup>



*Figure 14 Fracture vBMD vs.  $F_{PEAK}$  Scatterplot: No significant relationships between vBMD at fracture site 1 or  $F_{PEAK}$  ( $p=0.846$ ).<sup>1</sup>*

Before comparing the combination variable of SSI to the structural properties. It was essential to determine the relationships between  $Z$  and the structural properties alone.  $Z$  at the site of fracture was not normally distributed. To correct this error, the data were transformed using a consistent calculation of  $\log_{10}(Z \text{ variable})$  to achieve normality. Using linear regressions,  $Z$  demonstrated significant predictability to all structural properties ( $p<0.0001$ ). In fact, testing showed that  $Z$  was able to explain for 34.76% of the variation in  $U_{TOT}$ , 67.68% of the variation in  $F_{PEAK}$ , and 54.24% of the variation in  $K$ . (Figures 15, 16, 17)

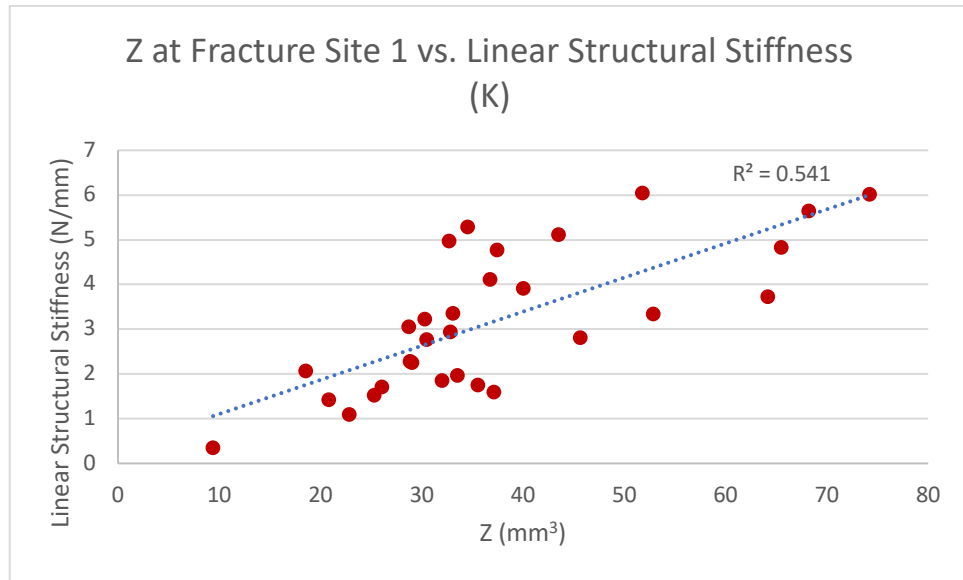


Figure 15 Z vs. K Scatterplot: Fracture site 1 Z was able to significantly predict K and accommodate for 54.24% of variation in the population sample ( $p < 0.0001$ ).<sup>1</sup>

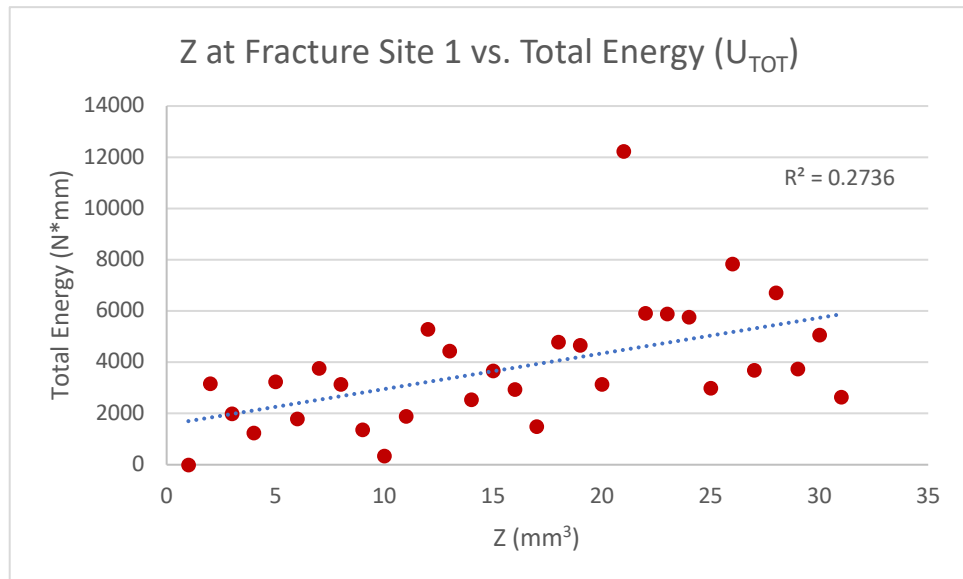
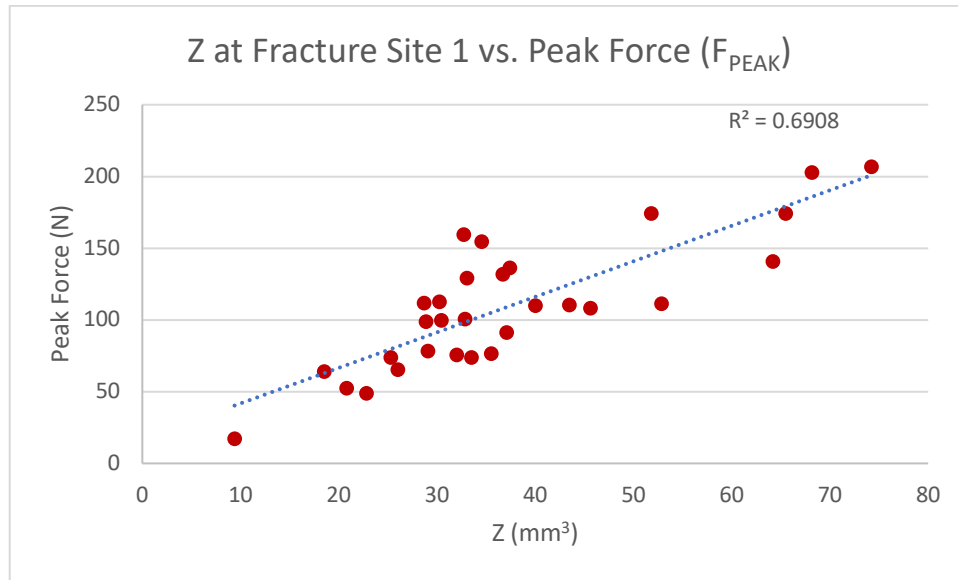


Figure 16 Z vs.  $U_{TOT}$  Scatterplot: Fracture site 1 Z was able to significantly predict  $U_{TOT}$  and accommodate for 34.76% of variation in the population sample ( $p < 0.0001$ ).<sup>1</sup>



*Figure 17 Z vs.  $F_{PEAK}$  Scatter plot: Fracture site 1 Z was able to significantly predict  $F_{PEAK}$  and accommodate for 67.68% of variation in the population sample ( $p < 0.0001$ ).<sup>1</sup>*

In order to create a multifactor parameter for testing SSI was created from the fracture site vBMD and the fracture site Z. When SSI was calculated it was not normally distributed. To correct this error, the data were transformed using a consistent calculation of  $\log_{10}(\text{SSI variable})$ . Once normalized, SSI demonstrated significant predictability for all three structural properties ( $p < 0.001$ ). In fact, SSI was able to predict and accommodate for large amounts of variation in the sample population for  $U_{TOT}$ ,  $F_{PEAK}$ , and K, 36.82%, 61.37%, and 45.80%, respectively. (Figures 18, 19, 20)

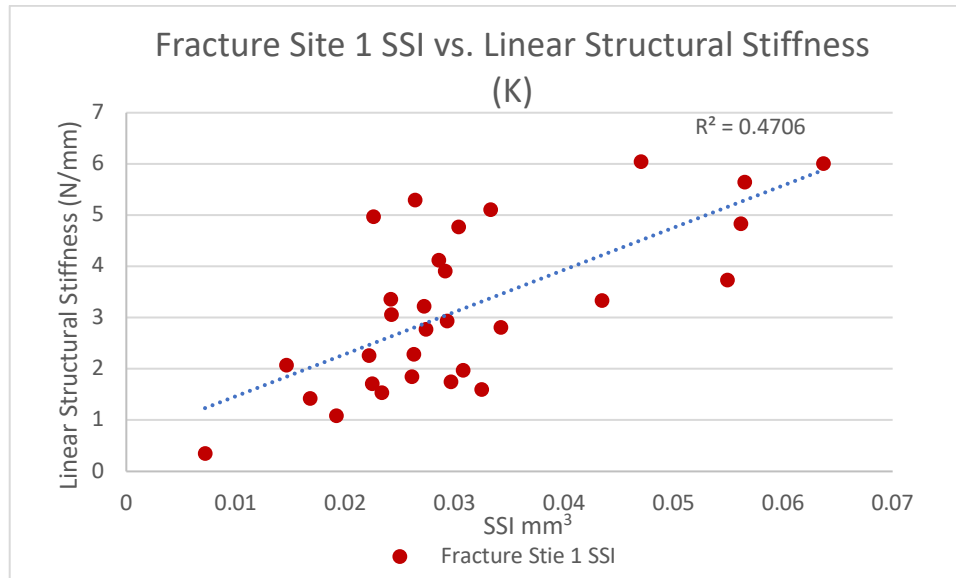


Figure 18 SSI vs. K Scatterplot: Fracture site 1 SSI was able to significantly predict K and accommodate for 45.80% of variation in the population sample ( $p < 0.001$ ).<sup>1</sup>

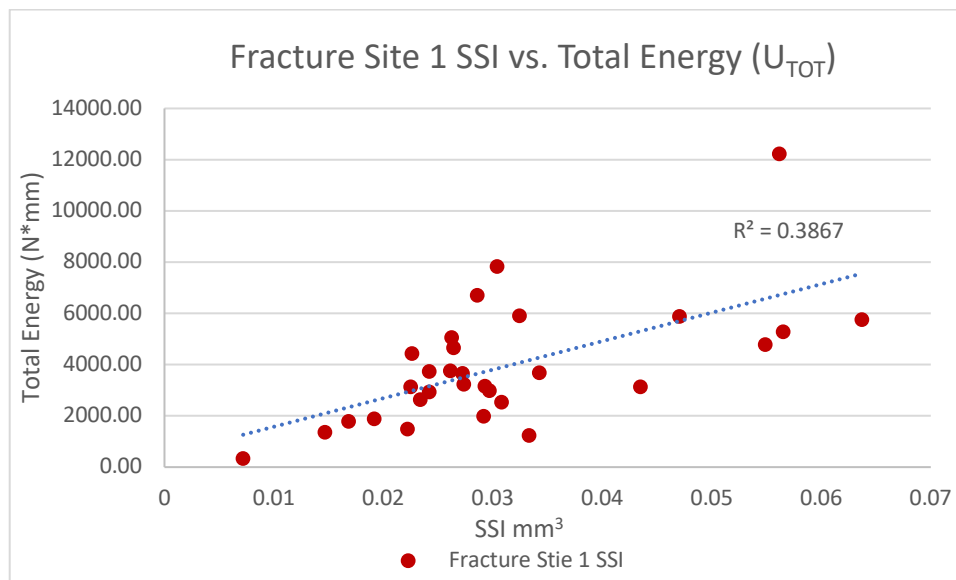
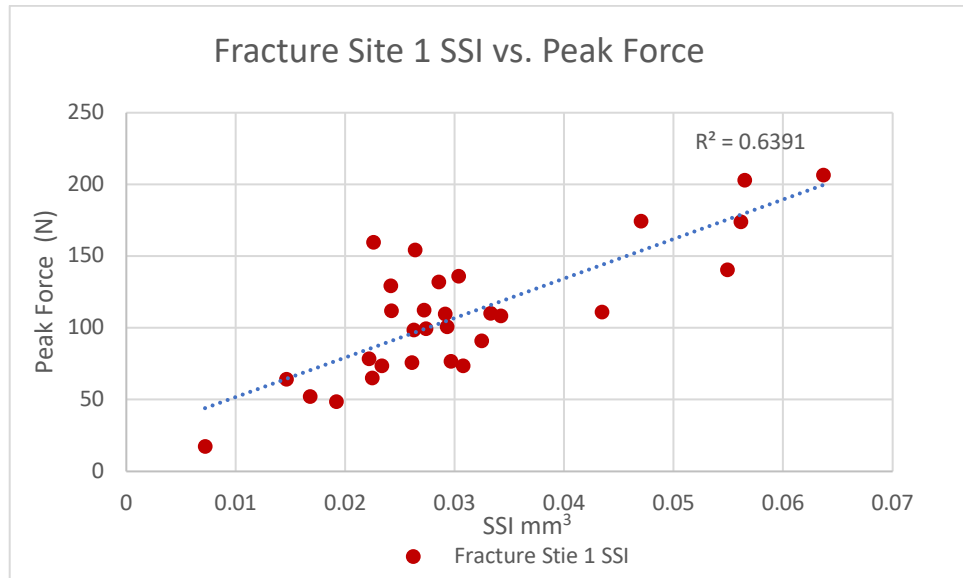


Figure 19 SSI vs.  $U_{TOT}$  Scatterplot: Fracture site 1 SSI was able to significantly predict  $U_{TOT}$  and accommodate for 36.82% of variation in the population sample ( $p < 0.001$ ).<sup>1</sup>





*Figure 20 SSI vs.  $F_{PEAK}$  Scatterplot: Fracture site 1 SSI was able to significantly predict  $F_{PEAK}$  and accommodate for 61.37% of variation in the population sample ( $p < 0.001$ )<sup>1</sup>*

## DISCUSSION

### *Variation of vBMD within the Rib*

The results from this study have proven to be insightful in multiple regards. In the *age-matched sample*, we were able to evenly distribute males and females to properly account for age and sex. With our results we can clearly see a declining trend in vBMD along the length of the rib from posterior to anterior. Variation within the rib itself suggests that intra-human variation contributes to rib bone quality and strength. Because DXA utilizes a generalized T-score to determine the average density of calcium hydroxyapatite, it is unable to depict subtle, but significant differences within the bone itself, making it unreliable and inaccurate in its bone quality assessment. This variation in vBMD within the rib suggests that other factors like it may also vary within the bone itself. Potentially these factors could even co-vary and demonstrate related distributions throughout the bone or inverse distributions, much like the inverse relationship between Z and vBMD in the tibiae.<sup>11</sup>

### *Overall lack of vBMD Predictability to Structural Properties*

The structural properties of the ribs give raw but useful data on the overall quality bone assessment. When the physical 2D Dynamic Loading Test was conducted on the *physically tested sample* we were able to collect data on how much force the bone could withstand, the total amount of energy, and even calculate its linear structural stiffness from the slope of the elastic portion on the force-displacement curve. Our results demonstrated that vBMD was not able to significantly predict these properties, biologically speaking, with the exception of the 30% site vBMD showing statistical significance in predicting  $F_{PEAK}$ . Even though the 30% site was able to predict  $F_{PEAK}$ , the amount of variation within the population sample that it was able to account

for was insignificant compared to the vast amounts of human variation within a global population. This shows differences in other studies such as Muller et al. (2003) found that aBMD from DXA scans were able to predict the fracture of the distal radius. Indications such as this suggest that intra-human variation from bone-to-bone should be considered when assessing bone quality and strength.<sup>17</sup>

### *Insignificance of Fracture Site vBMD to Structural Properties*

Calculating the fracture site vBMD was done to determine if vBMD at the point of fracture was able to significantly predict the structural properties. However, even though this is where the bone itself broke, it was unable to predict any of the structural properties related to the 2D Dynamic Loading Test. This suggests that some other factor or multiple factors are contributing to the overall fracture risk of the rib. While the statistical significance of these results was not close to becoming significant, it is possible that with a large sample size these results could change or stay the same. These same results were seen in a previous study conducted by Agnew et al. (2018). BMD scores demonstrated significant relationships to structural properties,  $U_{TOT}$ ,  $F_{PEAK}$ , and  $K$  ( $p < 0.0001$ ), however, BMD only predicted small portions of variation within the sample.<sup>1</sup> Indicating and reconfirming that BMD in general is not a good predictor of bone quality and its assessment.<sup>1</sup>

### *Analysis of Fracture Site Z and Structural Properties*

In contrast to Hunter et al. (2019), data demonstrated that  $Z$  was able to significantly predict structural properties obtained during the dynamic testing better than the combination variable of SSI, with the exception of  $U_{TOT}$ . While these findings demonstrate that vBMD may

lower SSI's effectiveness in predicting structural properties, it may be due to the smaller sample size, and varying locations of fracture in which Z and SSI were quantified. A larger sample size and obtaining more consistent variations of rib fracture locations may prove to be useful with further analysis of Z's comparative predictability to SSI.

### *Differences in Fracture Site SSI and Structural Properties*

In accordance with the results that were obtained by Hunter et al. (2019), data demonstrated that SSI was able to significantly predict structural properties,  $U_{TOT}$ ,  $F_{PEAK}$ , and K in the ribs which can easily be explained since SSI utilizes Z which significantly predicts structural properties in the rib in a large scale investigation by Agnew et al. (2018). In this study, we were able to confirm the results, from Agnew et al. (2018) and Hunter et al. (2019), with the SSI calculated from fracture site vBMD being able to predict  $U_{TOT}$ ,  $F_{PEAK}$ , and K due to the contribution of Z. In this study, Z significantly predicted structural properties  $U_{TOT}$ ,  $F_{PEAK}$ , K ( $p < 0.0001$ ) but SSI was able to predict more variance in the sample suggesting more than just one bone quality variable may be useful for future work.<sup>1</sup> Other studies, such as Muller et al. (2003) found that combination variables, much like the utilization of SSI in this project, explains far greater amounts in the sample being studied than just one single variable.<sup>17</sup> In fact, when combining geometric factors to BMD, Muller et al. (2003) found that the amount of variance that could be explained increased from 9% to 83% when predicting the failure of the bone, in this case the radius. Data collected in this study, with a reduced sample size compared to Muller et al. (2003), suggest that combination variables also demonstrate better predictability of the structural properties related to bone fracture.<sup>17</sup>

## *Overall Conclusions*

Thoracic injuries have the potential to result in the fatalities of patients involved in MVCs. Their fractures pose threats to highly vascular organs that are essential to sustaining human life. With intra-human variation detected in the vBMD of ribs, it is likely that one single parameter or score is of questionable value when attempting to predict and comprehensively assess total rib bone quality and strength. Even when accounting for variation in vBMD, only one vBMD site along the rib's length was able to significantly predict just one structural property. Even with its statistical significance, biologically it accounted for a small portion of the population sample.

Utilizing the vBMD from the actual location of fracture, it was thought that more predictability would result from this site. In actuality there was little evidence supporting that vBMD alone at this site can predict structural properties of the rib. To accommodate for this lack of predictability, a combination factor was utilized to demonstrate a factor that could predict more variation in the structural properties. As predicted, SSI was able to account for more variation when compared to the structural properties, reaffirming previous research done by Hunter et al. (2019), Agnew et al. (2018), and Muller et al. (2003), and suggesting that one variable alone, like vBMD, isn't enough when assessing bone quality.

The overall lack of conclusive predictability and the significant variations detected within the bone itself suggest that multiple factors and parameters are involved in defining bone quality and strength. Using combination factors may also prove useful when assessing the structural properties of bone and determining a more clinically useful methodology when defining bone quality, strength, and its relation to fracture. However more testing should be done to reconfirm SSI's ability to predict structural properties. Increasing sample sizes and determining variation in

other properties within the rib could help redefine and deepen our understanding our total bone quality assessment and fracture predictability. Further studies will need to be conducted to develop a more well-rounded understanding on how the data in this project and in others relates to redefining our concepts of total bone quality assessment.

## REFERENCES

1. Agnew A, Murach M, Dominguez V, et al. (2018) Sources of Variability in Structural Bending Response of Pediatric and Adult Human Ribs in Dynamic Frontal Impacts . *Stapp Crash Car Journal*. 2018;62:119-192.
2. Agnew, A. M., Schafman, M., Moorhouse, K., White, S. E., & Kang, Y. (2015). The effect of age on the structural properties of human ribs. *Journal of the Mechanical Behavior of Biomedical Materials*, 41. doi:10.1016/j.jmbbm.2014.09.002
3. Blake GM, Fogelman I. The role of DXA bone density scans in the diagnosis and treatment of osteoporosis. *Postgraduate Medical Journal*. 2007;83(982):509-517.  
doi:10.1136/pgmj.2007.057505
4. Bolotin, H. (2007). DXA in vivo BMD methodology: An erroneous and misleading research and clinical gauge of bone mineral status, bone fragility, and bone remodelling. *Bone*, 41(1).  
doi:10.1016/j.bone.2007.02.022
5. Brandi, M. L. (2009). Microarchitecture, the key to bone quality. *Rheumatology*, 48(Suppl 4), Iv3-Iv8. doi:10.1093/rheumatology/kep273
6. Clarke, B. (2008). Normal Bone Anatomy and Physiology. *Clinical Journal of the American Society of Nephrology*, 3(Supplement 3). doi:10.2215/cjn.04151206
7. Garg, M., & Kharb, S. (2013). Dual energy X-ray absorptiometry: Pitfalls in measurement and interpretation of bone mineral density. *Indian Journal of Endocrinology and Metabolism*, 17(2). doi:10.4103/2230-8210.109659
8. Holcombe, S. A., Hwang, E., Derstine, B. A., & Wang, S. C. (2018). Measuring rib cortical bone thickness and cross section from CT. *Medical Image Analysis*, 49, 27-34.  
doi:10.1016/j.media.2018.07.003

9. Hunt, H. B., & Donnelly, E. (2016). Bone Quality Assessment Techniques: Geometric, Compositional, and Mechanical Characterization from Macroscale to Nanoscale. *Clinical Reviews in Bone and Mineral Metabolism*, 14(3), 133-149. doi:10.1007/s12018-016-9222-4
10. Hudelmaier, M., Kuhn, V., Lochm, Ller, E. M., Well, H., Priemel, M., Link, T. M., & Eckstein, F. (2004). Can geometry-based parameters from pQCT and material parameters from quantitative ultrasound (QUS) improve the prediction of radial bone strength over that by bone mass (DXA)? *Osteoporosis International*, 15(5). doi:10.1007/s00198-003-1551-8
11. Hunter, R., Agnew, A., Murach, M., & Briley, K. (2017). Preliminary Investigation into the Co-variation of Cortical Geometric Properties and vBMD along the Length of the Tibia. *IRCOBI Conference 2017*, 17(101).
12. Hunter R., Kang Y., Briley K., Agnew A. (2019) Feasibility of volumetric bone mineral density (vBMD) to predict rib structural properties. *The American Association of Physical Anthropology*.
13. Jepsen, K. J. (2009). Systems analysis of bone. *Wiley Interdisciplinary Reviews: Systems Biology and Medicine*, 1(1). doi:10.1002/wsbm.15
14. Jepsen KJ, Evans R, Negus CH, et al. Variation in tibial functionality and fracture susceptibility among healthy, young adults arises from the acquisition of biologically distinct sets of traits. *Journal of Bone and Mineral Research*. 2013;28(6):1290-1300. doi:10.1002/jbmr.1879
15. Lien, Y., Chen, C., & Lin, H. (2009). Risk Factors for 24-Hour Mortality After Traumatic Rib Fractures Owing to Motor Vehicle Accidents: A Nationwide Population-Based Study. *The Annals of Thoracic Surgery*, 88(4). doi:10.1016/j.athoracsur.2009.06.002



16. Liu, Y., Hsu, J., Shih, T., Luzhbin, D., Tu, C., & Wu, J. (2018). Quantification of Volumetric Bone Mineral Density of Proximal Femurs Using a Two-Compartment Model and Computed Tomography Images. *BioMed Research International*, 2018. doi:10.1155/2018/6284269
17. Muller ME, Bouxsein ML, Webber CE. Predicting the failure load of the distal radius. *Osteoporosis International*. 2003;14(4):345-352. doi:10.1007/s00198-003-1380-9
18. Murach, M. M., Kang, Y., Goldman, S. D., Schafman, M. A., Schlecht, S. H., Moorhouse, K., . . . Agnew, A. M. (2017). Rib Geometry Explains Variation in Dynamic Structural Response: Potential Implications for Frontal Impact Fracture Risk. *Annals of Biomedical Engineering*, 45(9), 2159-2173. doi:10.1007/s10439-017-1850-4
19. Nelson, D. A., Barondess, D. A., Hendrix, S. L., & Beck, T. J. (2000). Cross-Sectional Geometry, Bone Strength, and Bone Mass in the Proximal Femur in Black and White Postmenopausal Women. *Journal of Bone and Mineral Research*, 15(10). doi:10.1359/jbmr.2000.15.10.1992
20. Schafman, M. A., Kang, Y., Moorhouse, K., White, S. E., Bolte, J. H., & Agnew, A. M. (2016). Age and sex alone are insufficient to predict human rib structural response to dynamic A-P loading. *Journal of Biomechanics*, 49(14). doi:10.1016/j.jbiomech.2016.09.030
21. Schlecht, S. H., & Jepsen, K. J. (2014). Corrigendum to “Functional integration of skeletal traits: An intraskeletal assessment of bone size, mineralization, and volume covariance” [Bone 56 (2013) 127–138]. *Bone*, 62, 69-70. doi:10.1016/j.bone.2014.01.024
22. Schlecht, S. H., Bigelow, E. M., & Jepsen, K. J. (2014). Mapping the natural variation in whole bone stiffness and strength across skeletal sites. *Bone*, 67. doi:10.1016/j.bone.2014.06.031

23. Seeman, E. (2008). Structural basis of growth-related gain and age-related loss of bone strength Proceedings of a satellite symposium held on the occasion of the EULAR Congress, Paris, France, June 13, 2008. *Rheumatology*, 47(Supplement 4).  
doi:10.1093/rheumatology/ken177
24. Seeman, E., & Delmas, P. D. (2006). Bone Quality — The Material and Structural Basis of Bone Strength and Fragility. *New England Journal of Medicine*, 354(21), 2250-2261.  
doi:10.1056/nejmra053077
25. Watts, N. B., Geusens, P., Barton, I. P., & Felsenberg, D. (2005). Relationship Between Changes in BMD and Nonvertebral Fracture Incidence Associated With Risedronate: Reduction in Risk of Nonvertebral Fracture Is Not Related to Change in BMD. *Journal of Bone and Mineral Research*, 20(12). doi:10.1359/jbmr.050814
26. World Health Organization Assessment of fracture risk and its application to screening for postmenopausal osteoporosis: technical report series 843. Geneva: WHO, 1994

## APPENDIX

Subject ID	Rib Side	Rib Level	Sex	Age
6054	L	7	m	83
6600	L	6	m	66
6673	L	6	m	73
6717	L	7	f	69
6767	L	7	f	35
6782	R	6	m	62
6878	L	6	m	57
6906	L	6	f	45
6989	R	6	f	57
7012	R	6	m	48
7039	R	6	m	25
7089	R	6	f	54
7120	R	6	f	65
7219	L	6	f	66
7253	L	6	m	50
7282	R	7	m	68
7312	L	6	f	36
7316	L	6	m	60
7320	R	6	f	57
7378	L	6	f	72
7385	L	6	m	55
7416	L	6	m	65
7417	R	6	f	61
7447	R	6	f	83
7458	L	6	m	34
L13-0130	R	5	f	25
L13-0216	L	7	f	26
L14-0210	L	7	f	24
L16-0189	L	6	f	30
L16-0204	R	6	m	25
L16-0228	L	6	m	18
L16-0291	R	6	m	39
L16-0303	R	6	f	24
L16-0314	L	6	m	22
L16-0321	R	6	m	24
L16-0347	R	6	m	35
L16-0378	L	5	f	47
L16-0477	L	6	f	16
L16-0517	L	6	m	45

Table 1: The demographic data of the age-matched sample.

Subject ID	Rib Side	Rib Level	Sex	Age
6600	L	6	m	66
6673	L	6	m	73
6878	L	6	m	57
6906	L	6	f	45
6989	R	6	f	57
7012	R	6	m	48
7039	R	6	m	25
7089	R	6	f	54
7120	R	6	f	65
7219	L	6	f	66
7253	L	6	m	50
7282	R	7	m	68
7312	L	6	f	36
7320	R	6	f	57
7385	L	6	m	55
7417	R	6	f	61
7458	L	6	m	34
L16-0189	L	6	f	30
L16-0204	R	6	m	25
L16-0228	L	6	m	18
L16-0291	R	6	m	39
L16-0303	R	6	f	24
L16-0314	L	6	m	22
L16-0321	R	6	m	24
L16-0347	R	6	m	35
L16-0414	R	6	m	19
L16-0477	L	6	f	16
L17-0038	L	5	m	13
LL016-7017	R	6	m	35
MC1610787F	L	6	f	50

Table 2: The demographic data of the physically tested sample.

Figure 21 SSI Calculation Equation

$$SSI = \frac{(vBMD * Z)}{1200}$$